

Calogero-like model without rearrangement symmetry

Miloslav Znojil^{a,b}

^aThe Czech Academy of Sciences, Nuclear Physics Institute, Hlavní 130, 250 68 Řež, Czech Republic, e-mail: znojil@ujf.cas.cz

^bDepartment of Physics, Faculty of Science, University of Hradec Králové, Rokitanského 62, 50003 Hradec Králové, Czech Republic

Abstract

Reinterpretation of mathematics behind the exactly solvable Calogero's A -particle quantum model is used to propose its generalization. Firstly, it is argued that the strongly singular nature of the Calogero's particle-particle interactions makes the original permutation-invariant Hamiltonian tractable as a direct sum $H = \bigoplus H_a$ of isospectral components which are mutually independent. Secondly, after the elimination of the center-of-mass motion the system is reconsidered as living in the reduced Euclidean space \mathbb{R}^{A-1} of relative coordinates and decaying into a union of subsets W_a called Weyl chambers. The mutual independence of the related reduced forms of operators H_a enables us to choose them non-isospectral. This breaks the symmetry and unfolds the spectral degeneracy of H . A new, multi-parametric generalization of the conventional A -body Calogero model is obtained. Its detailed description is provided up to $A = 4$.

Keywords

Calogero's A_N model; asymmetric two-particle barriers; exact solvability requirement; coloring of the Weyl chambers;

1 Introduction

The well known [1, 2, 3] quantum Hamiltonian

$$H^{(A)}(\omega, C) = - \sum_{i=1}^A \frac{\partial^2}{\partial x_i^2} + \sum_{i < j=2}^A \left[\frac{1}{8} \omega^2 (x_i - x_j)^2 + \frac{2C}{(x_i - x_j)^2} \right], \quad x_k \in \mathbb{R}, \quad C > -\frac{1}{4} \quad (1)$$

invented by Calogero [4, 5, 6] and written here in units $\hbar = 2m = 1$ plays an important methodical role in nuclear, atomic and molecular physics and in quantum chemistry [7]. It is a truly remarkable one-dimensional A -particle-chain *alias* linear-molecule model which combines the non-numerical solvability [8] with a nontrivial and multi-branched phenomenological relevance [9, 10]. Its symmetry with respect to the permutations of coordinates $x_k \in \mathbb{R}$ is accompanied by a fairly realistic shape of its two-body interaction potentials mimicking not only the expected asymptotic attraction but also a frequently encountered repulsion at short distances [11].

Equally strongly the impact of the model can be felt in mathematics. The wealth of related innovations ranges from the upgrades of the applications of Lie algebras [12, 13, 14] and of orthogonal polynomials [15, 16] up to the amendments of paradigms known as Wigner-Dunkl quantum mechanics [17, 18], quasi-Hermitian quantum mechanics [19, 20, 21, 22, 23, 24] or \mathcal{PT} -symmetric quantum mechanics [25, 26, 27, 28, 29, 30, 31].

In our paper we intend to propose a multiparametric but still exactly solvable generalization of model (1). For introduction it is sufficient to consider just the most elementary two-particle special case

$$H^{(2)}(\omega, C) = -\frac{\partial^2}{\partial x_1^2} - \frac{\partial^2}{\partial x_2^2} + \frac{1}{8} \omega^2 (x_1 - x_2)^2 + \frac{2C}{(x_1 - x_2)^2}, \quad (x_1, x_2) \in \mathbb{R}^2. \quad (2)$$

The well known additional merit of the model emerges after one defines the two new “relative-motion” *alias* Jacobi coordinates [3]

$$R = \frac{1}{\sqrt{2}}(x_1 + x_2), \quad X = \frac{1}{\sqrt{2}}(x_1 - x_2) \quad (3)$$

and after one manages to separate the center-of-mass motion [32, 33]. This leads to the reduction and replacement of the initial partial differential Schrödinger equation by another, ordinary differential bound-state problem in $L^2(\mathbb{R})$,

$$\left[-\frac{d^2}{dX^2} + \frac{1}{4} \omega^2 X^2 + \frac{C}{X^2} \right] \psi_n(X) = E_n \psi_n(X), \quad X \in \mathbb{R}, \quad n = 0, 1, \dots \quad (4)$$

The positive $X \in \mathbb{R}^+$ corresponds to the ordering $x_1 > x_2$ (with the first particle lying, on the real line \mathbb{R} , to the right from the second one) while the negative choice of $X \in \mathbb{R}^-$ represents our pair of particles as positioned inside a complementary half-plane of $(x_1, x_2) \in \mathbb{R}^2$ where $x_1 < x_2$.

The two half-lines $\mathbb{R}^\pm \subset \mathbb{R}$ may be called Weyl chambers. In the literature, such a name is used at any number of particles A . After the standard elimination of the center of mass [34, 35] the A -particle-coordinate space \mathbb{R}^A becomes reduced to its subspace \mathbb{R}^{A-1} . This is performed in full analogy with the $A = 2$ change of coordinates (3) so that at any higher $A > 2$, the space \mathbb{R}^{A-1} remains parametrized by the relative Jacobi coordinates [3, 36, 37].

In terms of the latter coordinates the singular repulsion enters the game and the reduced space becomes split, in a way generalizing the $A = 2$ case, into a union of $(A - 1)$ -dimensional Weyl chambers W_a , i.e., $\mathbb{R}^{A-1} = \bigcup W_a$. Unfortunately, a return to $A = 2$ and to the reduced Schrödinger equation (4) reveals the existence of a subtle mathematical problem, well known to all of the authors of textbooks. In a way emphasized, e.g., by Landau and Lifshitz [38], the short-range force $\sim X^{-2}$ is strongly singular in the origin so that the Calogero's system living on the real line \mathbb{R} becomes tractable as composed of two *completely dynamically independent* quantum systems living on the respective permutation-characterized Weyl-chamber half-lines $\mathbb{R}^- = W_{(\{12\})}$ or $\mathbb{R}^+ = W_{(\{21\})}$. All of the meaningful phenomenological predictions (i.e., say, of the structure of the spectrum or of the wave functions) are then encoded in any one of its Weyl chambers. In this sense, the reference to the “global” Hamiltonians (2) or (1) can be considered (perhaps, unintentionally) misleading.

Such an observation has several consequences, some of which will be explained and described in what follows. The presentation of our results will be preceded by a brief review of some of the basic properties of the most elementary conventional Calogero model in section 2. As a core and guide to our project, the “asymmetrization” preserving the solvability will be proposed there at $A = 2$. In subsequent section 3 the details of analogous asymmetrization will be described at $A = 3$. After transition to arbitrary A , our innovated Calogero-like model will finally be analyzed and discussed in the last two sections 4 and 5 and in Appendix.

2 Spectral degeneracy and its unfolding at $A = 2$

The $\mathcal{O}(x^{-2})$ singularity in Eq. (4) resembles the centrifugal term in the radial Schrödinger equation of a centrally symmetric harmonic oscillator in a specific ℓ -th partial wave. Formally, we may reparametrize $C = \ell(\ell + 1)$ and reconstruct the real (though, in general, non-integer and/or non-positive) angular-momentum-like parameter ℓ from a given value of coupling constant C ,

$$\ell = \ell(C) = -\frac{1}{2} + \sqrt{\frac{1}{4} + C}. \quad (5)$$

A decisive difference from the radial Schrödinger equation is that our present Eq. (4) has to live, by definition, on the whole real line of $X \in \mathbb{R}$. In the Calogero's operator $H^{(2)}$ of Eq. (2) the two particle coordinates x_1 and x_2 are independent variables so that one has to represent the motion

in both the left Weyl chamber $W_{\{\{12\}\}}$ of $X \in (-\infty, 0)$ and the right Weyl chamber $W_{\{\{21\}\}}$ of $X \in (0, \infty)$.

2.1 Singularity in the origin

Due to the singularity at $X = 0$ our reduced Hamiltonian is merely essentially self-adjoint [39]. In the origin some additional boundary conditions have to be imposed in order to make the problem mathematically well defined. An explicit specification of physics behind these boundary conditions is necessary. Only then one can speak about a consistent quantum theory and about a unique operator associated with the differential expressions of Eq. (1) or, at $A = 2$, of Eqs. (2) and (4).

In this light we will accept, at $A = 2$, the most common convention by which one requires

$$\psi_n(X) \sim X^{\ell+1}, \quad X \sim 0, \quad \ell > -1/2. \quad (6)$$

This is equivalent to the suppression of the dominant component $\sim X^{-\ell}$ of the wave function near the origin (see a few related comments in [40]). The Calogero's reduced symmetric-interaction Eq. (4) can be then perceived as living on the full real line. In spite of the presence of the barrier, the bound states are made well defined by constraint (6).

In a more consequent and more physics-oriented conceptual setting the interpretation of the role of the barriers is less clear. The tunneling between the two neighboring half-lines *alias* Weyl chambers is fully suppressed. One could speak about a direct sum of the two independent quantum systems. Moreover, once we recall the even-parity symmetry of the potential in (4), we have a full freedom of redirecting our attention from the model defined on the whole real line back to just one of the independent sub-models. Both of these sub-models are isospectral so that the spectrum of the complete system is doubly degenerate.

In many applications, people decide to ignore the impenetrability of the barrier (i.e., the absence of any meaningful contact between the subsystems) preferring the reference to the full-line Hamiltonian (1). Such a slightly manipulative decision is presented as well motivated by the possibility of working, mostly in the context of statistical physics, with the two alternative versions of the wave functions which are constructed as spatially symmetrized or antisymmetrized,

$$\psi_n^{(symm/antisymm)}(X) = \frac{1}{\sqrt{2}}[\psi_n(X) \pm \psi_n(-X)], \quad n = 0, 1, \dots \quad (7)$$

In spite of a complete absence of tunneling, the respective wave-function superpositions (7) are declared tractable as mimicking a system of two indistinguishable “bosons” (due to the Pauli-principle-simulating symmetry $\psi(-X) = \psi(X)$) or “fermions” (with the spatial antisymmetry sampling the fermionic statistics).

Due to the degeneracy in combination with the absence of tunneling one could equally well decide to consider some more sophisticated full-line requirements with, say, wave functions such

that $\psi(-X) = q\psi(X)$, $X > 0$ using an arbitrary complex $q \in \mathbb{C}$. Nevertheless, in spite of being acceptable mathematically, such a generalization is not used. In the overall pragmatic context of the applied quantum mechanics, even the two most elementary specifications of $q = \pm 1$ are believed to make the most elementary one-dimensional two-particle version (4) of the conventional Calogero model as well as all of its $A > 2$ descendants sufficiently appealing, intuitive and useful.

In our present paper we intend to advocate a different philosophy.

2.2 Asymmetric barrier

During the recent developments of quantum theory the Pauli-principle-rooted paradigm seems to be shattered. The first, purely mathematical reason is that once we have zero tunneling through the Calogero's barrier, there is no reason for keeping this barrier formally left-right symmetric. In Eq. (4) with $C = \ell(\ell + 1)$, therefore, we can feel free to "asymmetrize" the singular term,

$$\frac{\ell(\ell + 1)}{X^2} \rightarrow \begin{cases} \ell_{(left)}(\ell_{(left)} + 1)/X^2, & X < 0, \\ \ell_{(right)}(\ell_{(right)} + 1)/X^2, & X > 0, \end{cases} \quad \ell_{(left)} \neq \ell_{(right)}. \quad (8)$$

Precisely such an idea of asymmetrization of the impenetrable barrier at $A = 2$ served as an inspiration of our present paper.

The idea appeared supported, independently, by some very recent developments in applications. The necessity of working with an asymmetric singular barriers emerged, for example, in the context of relativistic quantum mechanics [41]. The presence of interactions containing an asymmetric impenetrable barrier has been found productive, especially for certain systems described by one-dimensional Dirac equations (cf. [42]). In another paper (cf. [43]) the same authors introduced and solved Dirac equation in which the impenetrable barrier has been kept left-right symmetric. The routine reduction of the equation led to an equivalent Schrödinger-type differential equation defined along the whole real line in which the effective $\mathcal{O}(x^{-2})$ barrier re-appeared in a manifestly asymmetric form of Eq. (8) (see also a few more comments on this topic in Appendix).

Let us now accept the idea and let us replace, in our reduced Calogero-Schrödinger equation (4), the conventional symmetric $\mathcal{O}(x^{-2})$ barrier by its two-parametric asymmetric generalization (8). Such a model (i.e., two decoupled radial harmonic oscillators with different angular momenta) is exactly solvable [44]. Its spectrum can be written in closed form,

$$E = 4k + 2\ell + 3, \quad k = 0, 1, 2, \dots, \quad \ell = \ell_{left} > -1/2 \quad \text{or} \quad \ell = \ell_{right} > -1/2. \quad (9)$$

The degeneracy as encountered when $\ell_{left} = \ell_{right}$ becomes, up to accidental confluences, removed when $\ell_{left} \neq \ell_{right}$.

Due to the simplicity of the model it becomes entirely straightforward to deduce the basic consequences. In a methodically motivated analysis let us consider, nevertheless, just a special

case of Eq. (8) in which the asymmetry is kept one-parametric and maximal,

$$\ell_{left} = \ell_{left}(y) = y, \quad \ell_{right} = \ell_{right}(y) = -y. \quad (10)$$

After we recall Eq. (4) and out-scale the inessential spring constant $\omega \rightarrow 2$ we arrive at a drastically asymmetric one-parametric toy-model potential

$$V(X, y) = \begin{cases} X^2 + y(y+1)/X^2, & X < 0, \\ X^2 + (y-1)y/X^2, & X > 0, \end{cases} \quad y = \text{real} \quad (11)$$

the shape of which is sampled here in Figure 1.

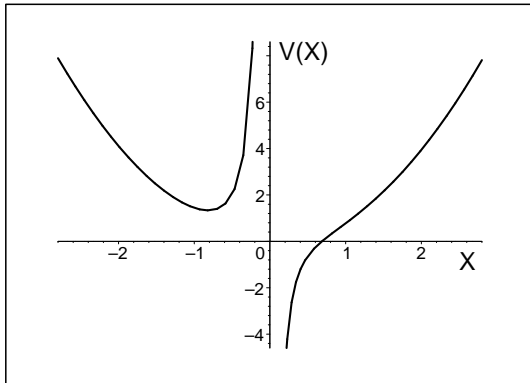


Figure 1: Potential (11) at $y = 1/3$.

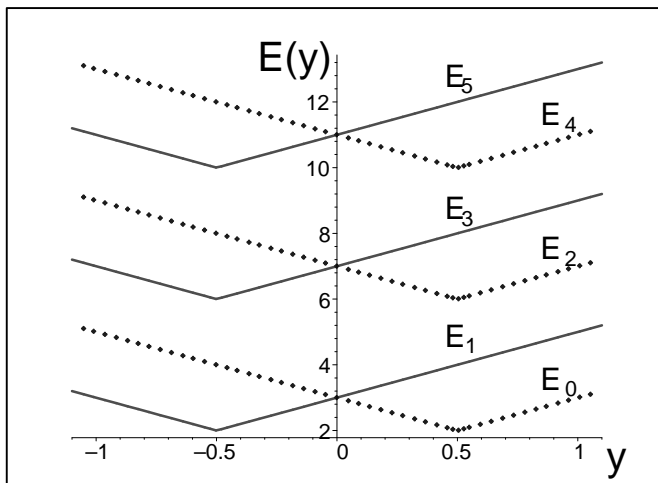


Figure 2: Bound-state energies in (11). Full/dotted lines mark the left-/right-well sub-spectra.

The explicit non-numerical form of the spectrum immediately follows from Eq. (9) and its y -dependence is displayed in Figure 2. The only instant of degeneracy occurs at $y = 0$. The spectrum even becomes equidistant at $|y| > 1/2$. One only has to add that the price to be paid for the unfolding of the degeneracy is in fact not too small:

Lemma 1 *Schrödinger Eq. (4) with one-parametric asymmetric potential (11) yields, at $y \neq 0$, the non-degenerate bound-state spectrum (9), but all of its “left” eigenfunctions $\psi_n(X)$ such that $X \in W_{\{12\}} = (-\infty, 0)$ vanish along the “right” Weyl-chamber half-line $W_{\{21\}} = (0, \infty)$ and vice versa.*

Analogous consequences can be drawn after the more general two-parametric asymmetrization of the barrier (cf. (8)), or after transition to a larger number of particles. With the details to be explained below, let us only mention here that once we, at any A , asymmetrize the boundary between some two Weyl chambers W_a and W_b by the choice of the respective couplings $C_a \neq C_b$, we reveal that in a way sampled by Lemma 1 and Figure 2, the composition of the two sub-spectra may remain non-degenerate. Up to the accidental degeneracies, therefore, the W_a -supported wave function ψ_a will necessarily vanish in W_b and *vice versa*.

In the limit of $C_a = C_b$ the spectrum becomes degenerate so that we may return to the wave-function superpositions as sampled by Eq. (7). Due to the absence of tunneling, there is still no reason for leaving the Weyl-chamber-dependent direct-sum interpretation of Hamiltonians (1).

We may now return to the two-body case in which the following statement is immediate.

Theorem 2 *After the asymmetrization (8) of the potential in Eq. (4), we merely have to replace the conventional two-parametric Calogero Hamiltonian of Eq. (2) by its three-parametric Weyl-chamber-dependent asymmetric-barrier generalization*

$$H^{(2)}(\omega, C_{(left)}, C_{(right)}) = \begin{cases} -\frac{\partial^2}{\partial x_1^2} - \frac{\partial^2}{\partial x_2^2} + \frac{1}{8} \omega^2 (x_1 - x_2)^2 + \frac{2C_{(left)}}{(x_1 - x_2)^2}, & x_1 < x_2, \\ -\frac{\partial^2}{\partial x_1^2} - \frac{\partial^2}{\partial x_2^2} + \frac{1}{8} \omega^2 (x_1 - x_2)^2 + \frac{2C_{(right)}}{(x_1 - x_2)^2}, & x_1 > x_2. \end{cases} \quad (12)$$

Strictly speaking the couplings $C_{(left)} = \ell_{(left)}(\ell_{(left)} + 1)$ and $C_{(right)} = \ell_{(right)}(\ell_{(right)} + 1)$ may though need not be different. In both of these scenarios the main message delivered by Theorem 2 is that if we wish to understand and to break the symmetry of the system (represented, in this section, by the $A = 2$ Hamiltonian $H^{(2)}(\omega, C)$ of Eq. (4)) and if we wish to introduce its consistently asymmetrized generalization (sampled, say, via Figure 1 above), we just have to take the two *different* versions of the Hamiltonian and we have to *restrict them* to the respective single Weyl chamber. In a way prescribed by Eq. (12), and in a way which will be generalized below: A similar conclusion will apply to the asymmetrized Calogero-like systems of more particles.

As long as the related analysis would be technically less transparent, it makes sense to proceed more slowly and to move, first, to the very next special case with three particles.

3 Spectral degeneracy and its unfolding at $A = 3$

For some purposes (and, in particular, for methodical purposes) the original symmetric Calogero model (1) as well as its present asymmetric Calogero-like generalization are too elementary at

$A = 2$. In both of these regimes, fortunately, the pedagogical merits of these models are only partially lost after transition to $A = 3$ [20].

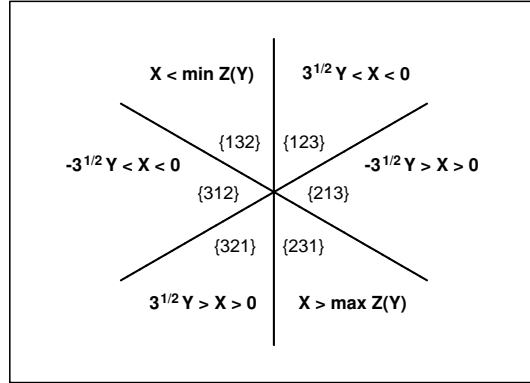


Figure 3: Six wedge-shaped Weyl chambers $W_{\{ijk\}}$ in $X - Y$ plane at $A = 3$.

3.1 Weyl chambers

In the Calogero's symmetric model (1) with $A = 3$ the change of variables

$$R = \frac{1}{\sqrt{3}}(x_1 + x_2 + x_3), \quad X = \frac{1}{\sqrt{2}}(x_1 - x_2), \quad Y = \frac{1}{\sqrt{6}}(x_1 + x_2 - 2x_3) \quad (13)$$

enables us to eliminate the center-of-mass motion and to arrive at the reduced but still partial differential Schrödinger equation in the $X - Y$ plane \mathbb{R}^2 ,

$$\left[-\frac{\partial^2}{\partial X^2} - \frac{\partial^2}{\partial Y^2} + \frac{3}{8}\omega^2(X^2 + Y^2) + \frac{C}{X^2} + \frac{C}{(\sqrt{3}Y - X)^2} + \frac{C}{(\sqrt{3}Y + X)^2} - E \right] \Phi(X, Y) = 0. \quad (14)$$

At any non-vanishing coupling constant $C > -1/4$ the three impenetrable barriers divide the plane into as many as six Weyl-chamber sectors. Their shapes are displayed in Figure 3. We define them there not only by the inequalities imposed upon X and Y (in which the symbol $Z(Y)$ stands for the set $Z(Y) = \{+\sqrt{3}Y, -\sqrt{3}Y\}$ of two elements) but also, equivalently, by the subscripts in $W_{\{ijk\}}$ which refer to the respective particle orderings $x_i < x_j < x_k$.

Another, third, equally ($A = 3$)-specific but formally independent definition of the Weyl chambers can be based on a spherical-coordinate reparametrization $X = \rho \sin \phi$ and $Y = \rho \cos \phi$ of the plane. After such a change of perspective our Calogero-Schrödinger Eq. (14) is found to be solvable by the separation of variables. This appeared to be a decisive discovery in [4] where the ansatz $\Phi(X, Y) = \psi(\rho)\chi(\phi)$ led to angular equation

$$\left(-\frac{d^2}{d\phi^2} + \frac{9C}{\sin^2 3\phi} \right) \chi_k(\phi) = \varepsilon_k \chi_k(\phi), \quad k = 0, 1, \dots \quad (15)$$

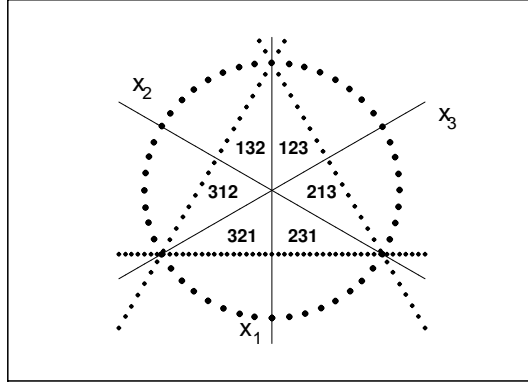


Figure 4: Weyl-chamber projections on the eye-guiding circle and triangle.

The impenetrable barriers of Figure 3 are now localized simply as lying along the constant-angle lines with $\sin 3\phi_{critical} = 0$.

The split of the two-dimensional plane into six Weyl chambers $W_{\{ijk\}}$ is presented, in a slightly modified manner, in Figure 4. The three solid lines of the preceding picture are reinterpreted as separating those subscripts of the Weyl chambers (i.e., those triplets of integers $\{ijk\}$) which only differ by a single elementary transposition. The line which represents the two-body repulsion barrier $\sim (x_1 - x_2)^{-2}$ and which stands for the transposition $1 \leftrightarrow 2$ is marked now by symbol “ x_3 ”, etc.

3.2 Non-equal barriers vs. loss of solvability

By far the most important formal merit of the conventional symmetric (i.e., equal-coupling) Calogero-Schrödinger Eq. (14) is that after the separation of variables, both the angular Eq. (15) and its more common harmonic-oscillator radial-equation partner prove solvable in closed form. This yields the spectrum

$$E = E_{n,k} = \sqrt{\frac{3}{8}}\omega (4n + 6k + 6\alpha + 5), \quad \alpha = \frac{1}{2}\sqrt{1 + 4C} > 0, \quad n, k = 0, 1, \dots \quad (16)$$

exhibiting multiple accidental degeneracies plus, in addition, a global sextuple degeneracy reflecting the split of the $X - Y$ plane in the six dynamically independent Weyl chambers. In this sense, every energy level of Eq. (16) can be assigned six independent wave functions. Due to the impenetrability of the barriers, every one of these functions may be chosen as exclusively supported by one of the eligible Weyl chambers,

$$\Phi = \Phi_{n,k}^{\{ijk\}}(X, Y) \begin{cases} \neq 0 & \text{for } (X, Y) \in W_{\{ijk\}} \\ = 0 & \text{otherwise.} \end{cases} \quad (17)$$

In opposite direction one could argue that the admissibility of the choice (17) (where the index ijk runs over all six permutations of triplet 123) is a consequence of the impenetrability of the Weyl-chamber boundaries. Implying that every one of the levels $E_{n,k}$ of Eq. (16), “locally” (i.e., inside W_a) degenerate or not, is also six times degenerate, in addition, “globally” (i.e., inside \mathbb{R}^2).

Let us now remind the readers that our present project is aimed, first of all, at an unfolding of the “global” spectral degeneracy. The goal is to be achieved by means of an asymmetrization of the Hamiltonian. In the $A = 3$ special case one of our guiding ideas is that the strength of the singularities of Hamiltonian (1) is only controlled by a single coupling constant C .

Preliminarily, one of the most natural tentative generalizations of model (14) might be sought via an *ad hoc* replacement of the single coupling constant C by a triplet of independent parameters,

$$\frac{C}{(\sqrt{3}Y - X)^2} \rightarrow \frac{Z_1}{(\sqrt{3}Y - X)^2}, \quad \frac{C}{(\sqrt{3}Y + X)^2} \rightarrow \frac{Z_2}{(\sqrt{3}Y + X)^2}, \quad \frac{C}{X^2} \rightarrow \frac{Z_3}{X^2}. \quad (18)$$

The denominators in (18) and, hence, also the localization of all of the Weyl-chamber boundaries would remain the same. In combination with the loss of symmetry, their impenetrability would imply the loss of the coincidence of the six Weyl-chamber-related sub-spectra $\{E_{n,k}^{\{ijk\}}\}$.

As long as the potentials inside the chambers can be now treated as a set of independent, isolated two-dimensional quantum dots, only the accidental “local” degeneracy between the bound-state sub-spectra will survive.

Remark 3 *The sextuple degeneracy of the energy levels (16) can be unfolded using the three-parametric asymmetrization (18) of the reduced Calogero-like Schrödinger Eq. (14). In such a case, the standard proof of the exact solvability of the model will not apply. In the future, indeed, the system might still be found solvable. On the present level of knowledge, unfortunately, the full exact solvability has to be declared, with all probability, lost.*

Incidentally, the latter methodical uncertainty may be related, perhaps, to the well known fact that in several generalized Calogero-type models the not quite expected exact solvability has been found as restricted to a *finite* subset of certain anomalous, “anharmonic” bound states [45]. A connection of such an incomplete, “quasi-exact” form of solvability with our present approach is nontrivial. Although the possible comparisons already lie beyond the scope of our present study, interested readers may find more details and inspiration, say, in the comprehensive review paper [46] published, in 2005, as a part of the Birthday Issue dedicated to Francesco Calogero on the occasion of his 70th birthday.

Another observation related to Remark 3 is that up to an accidental occurrence of a degeneracy, and in a sharp contrast to the symmetric scenario, virtually all of the bound states of the asymmetric model with unfolded spectrum will *necessarily* have to obey the single-chamber-support restriction (17) imposed upon wave functions.

3.3 Reinstallation of solvability: Asymmetric barriers

The validity and constructive nature of Theorem 2 at $A = 2$ might and have to be extended to all of the models with $A > 2$. In particular, the degeneracy of the Calogero's $A = 3$ spectrum has to be unfolded. Obviously, this degeneracy can be attributed to the particle-permutation symmetry of the Hamiltonian. Thus, as long as we wish to weaken the degeneracy in a way different from the preceding tentative recipe (18), we have to find another method of breaking that symmetry.

Naturally, we wish to do so without the loss of the exact, closed-form solvability of the original symmetric model. The overall strategy of so-doing has already been indicated above. We have to pick up six different coupling strengths $C_{\{ijk\}}$ and introduce six reparametrized versions of the Calogero's exactly solvable Hamiltonian of Eq. (1), $H \rightarrow H_{\{ijk\}} = H^{(3)}(\omega, C_{\{ijk\}})$. Now, although all of these operators are defined over the whole, unrestricted range \mathbb{R}^2 range of the coordinates, the impenetrability of the barriers enables us restrict their respective actions to the functions over a single Weyl chamber.

In this manner, we managed to complement the properly asymmetrized $A = 2$ model (12) by its exactly solvable $A = 3$ descendant.

Theorem 4 *Calogero-like quantum system with Hamiltonian*

$$H^{(3)}(\omega, \vec{C}) = \bigoplus_{\{ijk\}} H^{(3)}(\omega, C_{\{ijk\}}) \quad (19)$$

where

$$H^{(3)}(\omega, C_{\{pqr\}}) = - \sum_{m=1}^3 \frac{\partial^2}{\partial x_m^2} + \sum_{m < n=2}^3 \left[\frac{1}{8} \omega^2 (x_m - x_n)^2 + \frac{2C_{\{pqr\}}}{(x_m - x_n)^2} \right], \quad x_p < x_q < x_r. \quad (20)$$

is exactly solvable.

Proof. Such a model is a direct sum over all six permutations of integers $\{123\}$. Every one of its independent components (20) is obtained from the conventional model (1) after the elimination of the center-of-mass degree of freedom. Hence, up to the loss of the “global” degeneracy, the bound-state solutions remain “locally” unchanged even after the range of coordinates gets restricted from \mathbb{R}^{A-1} to $W_{\{pqr\}}$, and after the coupling is chosen equal to $C_{\{pqr\}}$. \square

Six independent coupling constants $C_{\{pqr\}}$ in Eq. (20) (*alias* the “colors” of the chambers) may but need not be all mutually different. Serving for an exhaustive classification of all of the asymmetric generalizations of the symmetric model. The classification can be given the form of a list of all of the possible nontrivial colorings of the six wedges in Figures 3 or 4.

As long as the explicit formulation of the list of the colorings is conceptually elementary, it may be left to the readers. Let us only note that besides the original Calogero's fully symmetric case

(using just a single color C) and besides the maximally asymmetric six-color system admitting a maximal reduction of the degeneracy, some of the other special colorings might also prove to be of an enhanced interest in applications. For example, we could be interested in the form of boundaries between the neighboring Weyl chambers $W_a \subset \mathbb{R}^2$ and $W_b \subset \mathbb{R}^2$. The reason is that these boundaries in \mathbb{R}^2 are just pull-downs of the microscopic particle-particle repulsion-force singularities in \mathbb{R}^3 . Various “realistic” sub-classifications might be then motivated by the need of being given a phenomenological input knowledge of dynamics on the microscopic level, with the emphasis put upon the difference between the symmetric barriers (when $C_a = C_b$) and their asymmetric repulsion-force alternatives (when $C_a \neq C_b$). Thus, in particular, whenever only some of the particle-particle barriers remain symmetric, we could speak about hybrid models. In these cases, the unfolding of the “global” spectral degeneracy would be just partial.

Alternatively one could demand that even when *all* of the particle-particle barriers become left-right asymmetric, the breakdown of symmetry may be incomplete, leading again to the mere partial removal of the model’s spectral degeneracy. Once we recall Figure 4 such an arrangement might be immediately visualized via coloring(s) in which one only uses a minimum (i.e., say, two) different colors. In these cases, the wave function of the system can (i.e., are allowed to) remain non-vanishing in more than one Weyl chamber, i.e., in principle, in the whole union of all of the Weyl chambers carrying the same color.

4 Spectral degeneracy and its unfolding beyond $A = 3$

4.1 Exact solvability

The systems with different A s will share formal analogies. In all of them, in particular, the Weyl chambers may be numbered by the configurations *alias* permutations of the particles. We will abbreviate $a = \{i_1, i_2, \dots, i_A\}$ and denote W_a if and only if $x_{i_1} < x_{i_2} < \dots < x_{i_A}$. Next, the singularities will occur, in \mathbb{R}^A , whenever $x_i = x_j$. After we eliminate the center of mass [33], these singularities will cut and split also the reduced space \mathbb{R}^{A-1} into its Weyl-chamber subsets W_a . The points of their boundaries ∂W_a are precisely the points at which the microscopic particle-particle interaction becomes singular.

For all of these reasons, many above-mentioned $A = 3$ considerations can be generalized to any A . In particular, the generalizations of Eq. (19) and of Theorem 4 to any A are immediate.

Theorem 5 *At any integer $A \geq 2$, the Calogero-like quantum system with Hamiltonian*

$$H^{(A)}(\omega, \vec{C}) = \bigoplus_{\{i_1 i_2 \dots i_A\}} H^{(A)}(\omega, C_{\{i_1 i_2 \dots i_A\}}) \quad (21)$$

where

$$\begin{aligned}
& H^{(A)}(\omega, C_{\{p_1 p_2 \dots p_A\}}) = \\
& = - \sum_{m=1}^A \frac{\partial^2}{\partial x_m^2} + \sum_{m < n=2}^A \left[\frac{1}{8} \omega^2 (x_m - x_n)^2 + \frac{2C_{\{p_1 p_2 \dots p_A\}}}{(x_m - x_n)^2} \right], \quad x_{p_1} < x_{p_2} < \dots < x_{p_A} \quad (22)
\end{aligned}$$

is exactly solvable.

At any A , in other words, the ultimate asymmetrized Calogero-like Hamiltonian remains formally defined as a direct sum of its mutually non-interacting particle-ordering-dependent components. Every such a model remains solvable. Even the limiting transition to the symmetric special case will be smooth.

The only remaining open problem seems to be the formulation of an explicit list of all of the structurally non-equivalent colorings $C_{\{p_1 p_2 \dots p_A\}}$. Thus, the qualitative characterization of the set of the repulsive-barrier coupling constants is a crucial task. Obviously, the task requires just a manageable visualization of the $(A - 1)$ -dimensional space of the relative coordinates after its decomposition $\mathbb{R}^{A-1} = \bigcup W_a$.

In such a framework, we are now prepared to give our preceding result an alternative formulation.

Theorem 6 *At any A , the exact solvability of the symmetric or asymmetric Calogero-like model of Eqs. (1) or (21) can be achieved via an explicit specification of the couplings $C = C_a$ which must only be the same at all of the inner sides of the boundaries of W_a .*

This observation provides the background and reason why our preceding constructive analyses are instructive and have to be complemented by their extension beyond $A = 3$.

In our ultimate illustration the choice of $A = 4$ does really form a certain “feasibility bridge” connecting the easy models where $A! \leq 6$ with the overcomplicated ones where $A! \geq 120$. Thus, it makes sense to show that also the four-particle Calogero-like asymmetrized models of Eq. (21) admit a feasible, compact and more or less explicit descriptive analysis.

4.2 Weyl-chamber boundaries and their cartography at $A = 4$

One of the key formal advantages of the conventional as well as generalized Calogero-like models with $A \leq 3$ is the separability of the initial partial differential Schrödinger equation, i.e., its reducibility to a set of ordinary differential eigenvalue problems. Such a feature is lost at $A \geq 4$ so that the simplest elements of this class with $A = 4$ deserve our constructive attention. Moreover, in a way advocated in the literature the choice of $A \leq 3$ as made in the two preceding sections need not be sufficiently representative, in a broader methodical context at least [47, 48]. As we already mentioned, the enumeration of the colorings in Figures 3 or 4 is next to trivial. We found it desirable to extend our discussion beyond $A = 3$, therefore.

4.2.1 Colorings at $A = 4$.

At $A = 3$ the task of the split of the plane \mathbb{R}^2 by the sextuplet of the wedge-shaped Weyl chambers as well as the related classification *alias* coloring problems were comparatively easy to settle. *All* of the half-line Weyl-chamber boundaries shared a common vertex and formed a planar star. This made the coloring of the wedges $W_{\{ijk\}}$ easy, leading immediately to an exhaustive classification of all of the unfoldings of the degeneracies, i.e., of all of the spectrally non-equivalent models. Moreover, it appeared sufficient to classify just the colorings of the six segments of an auxiliary circle or, equivalently, of an auxiliary triangle (cf. Figure 4).

The situation at $A = 4$ is perceptibly more complicated. Indeed, we have to replace, first of all, the $A = 3$ change of variables (13) by its $A = 4$ analogue. Nevertheless, the details of the $A = 4$ change of variables as well as an explicit discussion of a deep algebraic discussion of its consequences will be skipped here, for three reasons. Besides the first one (viz., the sake of brevity: their form is well known) and the second one (viz., a redundancy for our present purposes: the algebraic $A = 4$ formulae already become far from transparent), our third and main reason is that in a way sampled by Figure 4 at $A = 3$, it will be *sufficient* to know only the topology (i.e., the neighborhoods) of the $A = 4$ Weyl chambers. *Just* in its graphical form.

4.2.2 Projection on a central sphere.

Interested readers may find a deeper insight in the formulae and multiple deep algebraic structures in the dedicated literature [3, 49, 50]. At $A = 4$, in particular, one suddenly has to deal with as many as $A! = 24$ eligible Weyl chambers. Thus, a replacement of the formulae by their graphical alternatives seems well founded. It enhances, indeed, the efficiency of the analysis. In particular, the description becomes facilitated when we recall and adapt the graphical tricks as used at $A = 3$. In the first step, the centralized dotted-curve auxiliary planar circle of Figure 4 can be replaced, at $A = 4$, by a sphere in three dimensions.

Interested readers are encouraged to find a nice picture of such a sphere on the web [51]. In this representation one can also keep the analogy with the planar case of Figure 4 and project the three-dimensional objects $W_{\{ijkl\}}$ on the spherical triangles as displayed on the sphere in [51].

4.2.3 Projections on a central cube.

The role of the dotted-line triangle of Figure 4 can readily be transferred, at $A = 4$, to a central tetrakisshexahedron of Ref. [52]. A key advantage of such an upgrade of projection is that it further simplifies the representation. It replaces the projections of the three-dimensional Weyl chamber pyramids $W_{\{ijkl\}}$ on the spherical triangles by the flat, planar triangles of the surface of the tetrakisshexahedron of Ref. [52].

Although the colorings of the planar triangular faces of the tetrakisshexahedron look already feasible, let us still introduce another, last simplification converting the tetrakisshexahedron of Ref. [52] into a cube, with its six faces divided into quadruplets of the neighboring W_a —representing triangles. For completeness, interested readers can find the three-dimensional picture of such a cube with subdivided faces on internet [53]. In Figure 5 we present here its planar, two-dimensional unfold.

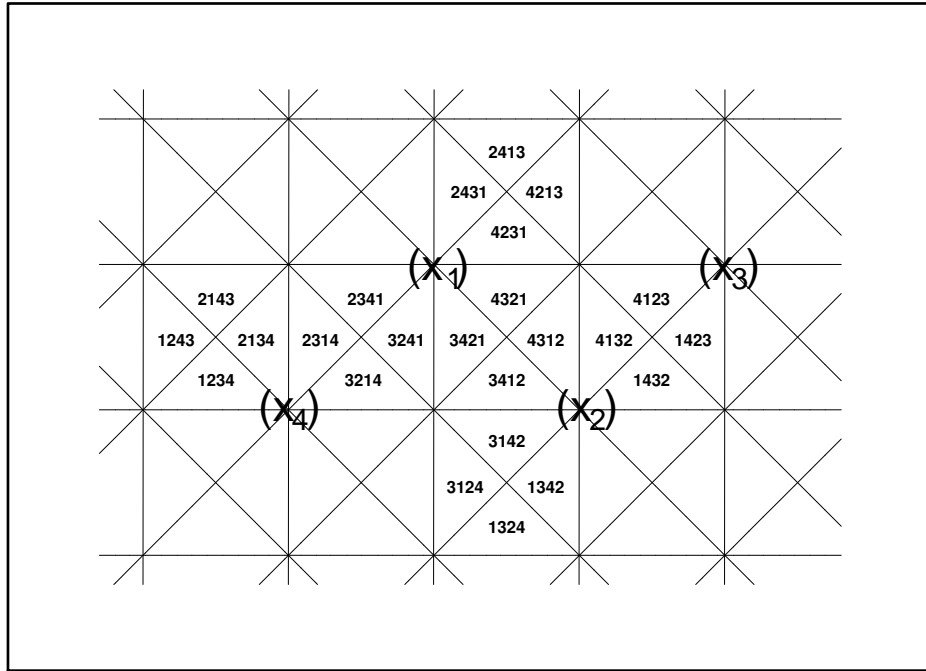


Figure 5: Twenty four Weyl chambers $W_{\{ijkl\}}$ in projection on a central cube.

4.2.4 Numbering by permutations.

For our present purposes we may cut and display the surface of the cube in the planar-cartography representation of Figure 5. We only have to remember that such a planar picture might require, for some purposes, a reconstruction of the three-dimensional surface of the cube by bending and gluing some of the edges.

The union $\mathbb{R}^{A-1} = \bigcup W_a$ has to be taken over all of the permutations of the particles. It is only important for us to know that *before* the projection as sampled in Figure 5 the geometric shape of the individual three-dimensional $A = 4$ Weyl chambers $W_{\{ijkl\}}$ will have again the pyramidal form, with their top fixed in the origin. We may expect that in comparison with the three-particle model, the generalization of the “cartography” to $A = 4$ (and, in principle, to any larger $A > 4$) is straightforward.

After the projection on the cube we have to deal with the planar representation of the surface. The vertices of the cube coincide with the intersections of the six singularity lines (i.e., of the three lines standing for the adjacent edges and of the other three ones for the face diagonals). One only has to remember that these vertices were defined as the octuplet of points in \mathbb{R}^3 at which the circumscribed auxiliary sphere is intersected by the four straight lines representing the original particle-coordinate axes of x_1, x_2, x_3 and x_4 . These intersections are also identified in Figure 5.

In this picture the surface of the inscribed cube is represented by the six concatenated squares. The symbols (x_j) mark the intersections of outwards-running axes with the sphere and with the cube (at its vertices). The planar triangular projections of all of the twenty four three-dimensional Weyl chambers $W_{\{ijkl\}}$ on the walls of the cube are finally numbered here by the quadruplets $ijkl$ of integers such that $-\infty < x_i < x_j < x_k < x_l < \infty$. In this manner we obtained again a transparent schematic two-dimensional representation of the Calogero-model kinematics at $A = 4$.

In the same picture the straight lines mark the singularities (i.e., the barriers) and the numbers $ijkl$ characterize the (projections of the) $A = 4$ chambers $W_{\{ijkl\}}$. One can easily check that whenever one crosses the line, the quadruplet of integers $ijkl$ is changed just by an elementary permutation of its neighboring elements. This permutation (i.e., a re-arrangement of the particles) can be perceived as a consequence of the crossing of the barrier *alias* singularity line.

As a serendipitous byproduct of these topological considerations we may deduce the following, not quite expected combinatorial result.

Lemma 7 *Once we localize the positive half-line intersections x_1, x_2, x_3 and x_4 on the auxiliary cube's surface, the allocation of the permutations $ijkl$ to the triangles of the cube's surface is unique.*

This observation returns us to the model with $A = 3$ where we marked, in Figure 4, also the projections of the triplet of the original Cartesian particle-coordinate axes x_1, x_2 and x_3 . These lines intersected the auxiliary circle at the six “barrier-sampling” points. At $A = 4$ the idea remains applicable because now, the intersections of the sphere with the axes x_1, x_2, x_3 and x_4 form an octuplet of the “marked” points in the diagram of Figure 5.

We may identify the latter points with the vertices of our auxiliary cube defined as inscribed in the auxiliary sphere. This enables us to project the boundaries of the separate Weyl chambers on the walls of the cube yielding the singularity lines in Figure 5. Summarizing, the twenty four Weyl chambers are mapped on the set of spherical triangles covering the auxiliary sphere. They are, incidentally, rectangular. Their planar projections cover the surface of the above-mentioned inscribed cube, with the rectangularity preserved. What is important is that the one-to-one correspondence between the topology of the three-dimensional Weyl chambers and the topology of the “numbered” triangles in Figure 5 is achieved and guaranteed.

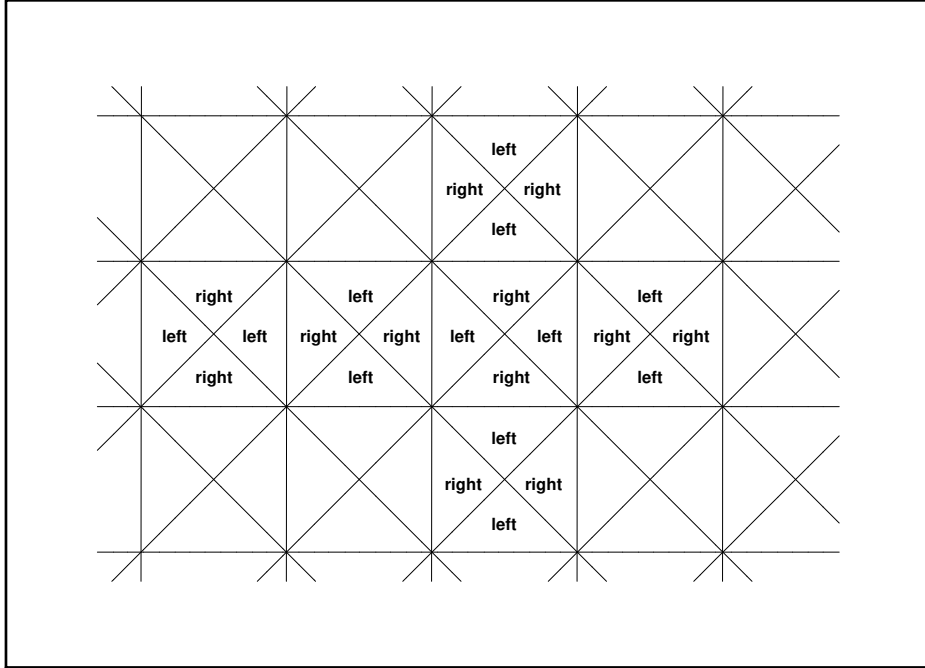


Figure 6: The $A = 4$ coloring with unique (viz., left-right) asymmetry of *all* of the barriers.

4.3 Alternative cartography at $A = 4$

Let us repeat that after a routine elimination of the center-of-mass degree of freedom the $A = 4$ constructions have to be simplified by the reduction of the initial partial differential Schrödinger equation in four coordinates to its three-dimensional effective version [37]. As long as we are mainly interested in the structure of the decomposition of \mathbb{R}^3 into a union of the Weyl chambers, we will not need the explicit formulae for the wave functions. These formulae may already be fairly complicated, see [3, 54]. Fortunately, our present task is just the specification of the Weyl chamber or chambers W_a in which the wave function of a relevant bound state can be nontrivial, $\psi_a \neq 0$.

Such a specification should be based on a visualization of the decomposition of \mathbb{R}^3 and on the phenomenologically motivated assignment of the equal or different couplings $C = C_a$ to the respective chambers $W = W_a$ at all of the position permutations $a = \{i_1, i_2, i_3, i_4\}$. Naturally, an exhaustive and systematic account of all of the possibilities would already be too long. For a selection of a sample we propose to combine a “minimal” nontrivial coloring (using just two colors $C = C_{left} \neq C_{right}$) with a “maximal” asymmetry of the barriers (meaning that none of the barriers $\sim (x_i - x_j)^{-2}$ remains symmetric, i.e., invariant under the exchange of particles $x_i \longleftrightarrow x_j$). A sample of the maximally asymmetric arrangement (using just two colors called “left” and “right”) is displayed in Figure 6.

4.3.1 Projections of the set of Weyl chambers on tetrahedron

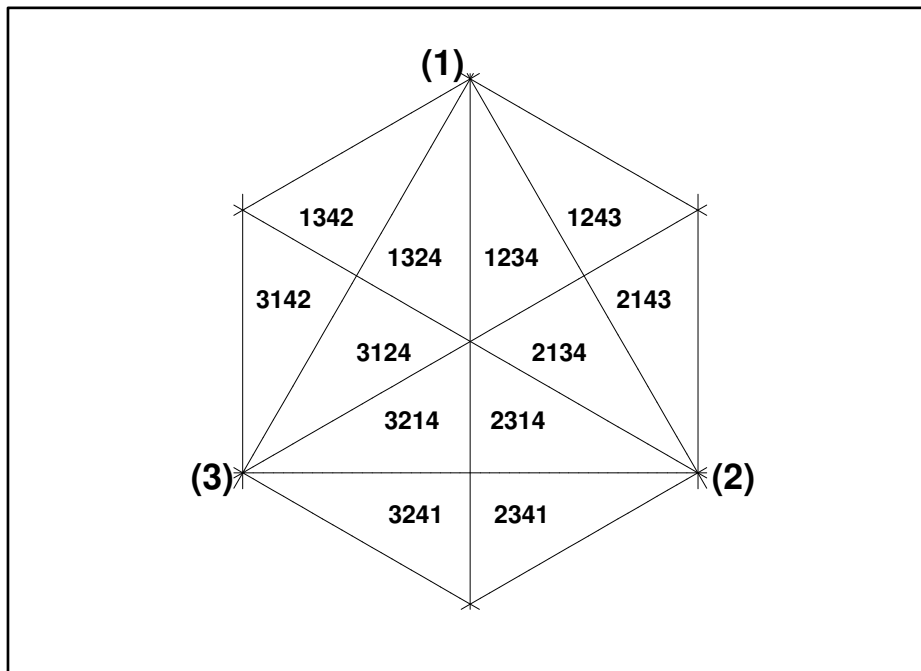


Figure 7: The upper half of the auxiliary cube of Figure 5 as seen from vertex “ (x_4) ”.

The surface of the cube of preceding paragraph is a three-dimensional object. Its cut and straightening were used yielding Figures 5 and 6. An alternative approach to the visualization of the same three-dimensional cube is sampled in Figure 7 where just half of its surface is presented as seen after the cube is rotated in such a way that the vertex marked by symbol “ (x_4) ” appears in front and in the very center of the picture.

Although the latter planar view represents the three-dimensional cube, we might re-read the same picture as a flat triangle with vertices (1), (2) and (3), endowed with the three planar extensions which could be bent along the edges and turned down. A new three-dimensional surface emerges. Its complementary, “invisible” lower half could be reconstructed, given the same shape and glued to the upper half.

Admissibly, such a type of reconstruction of the missing part of Figure 7 is oversophisticated. Nevertheless, just its minor reinterpretation yields another, much more regular Platonic-body representation of the topology, i.e., of the representation of the Weyl-chamber neighborhoods. Explicitly it is presented in Figure 8. The Weyl chambers (numbered there by the mere triplets of integers) are organized there into three triangles. The upper one (with vertices (1), (2) and (3)) has to stay unchanged while the other three triangles have to be all bent down, with their respective circle-marked “outer” vertices A , B and C to be glued together. Forming the fourth vertex of a tetrahedron which should be endowed with symbol (4).

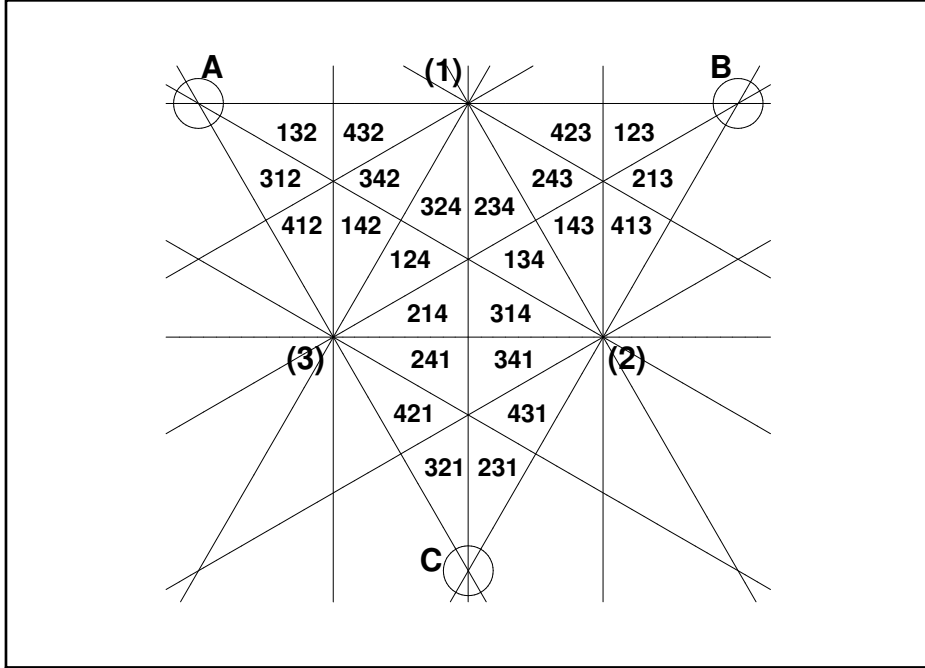


Figure 8: A tetrahedral alternative to Figure 5 (the surface unfolded into triangle ABC).

In Figure 8 the three intersections marked as (1), (2) and (3) have to be interpreted as the three vertices of one of the four triangular sides of an auxiliary central tetrahedron. Its remaining three sides are triangles (1) B (2), (2) C (3) and (3) A (1). In the picture the surface of the tetrahedron is unfolded so that after its refolding (in three dimensions) the three “outermost” vertices of the large triangle (marked by the small circles and by the letters A , B and C) will coincide.

In a marginal remark let us add that for the sake of brevity we numbered all of the small, Weyl-chamber-representing triangles just by the triplets of integers jkl . The reason is that for a return to the full-fledged notation $W_{\{ijkl\}}$ the “missing” value of i is provided by the nearest vertex (i). The rule becomes sufficient after the symbols A , B and C are all re-read as (4). Incidentally, in such a simplification we can move one step further. This is explained in our last Figure 9 in which we attached the new quadruplet of symbols $[l]$ to the remaining four vertices. Then, as long as all of the neighboring Weyl-chambers $W_{\{ijkl\}}$ share the last integer l with the vertex $[l]$, just two digits suffice for the labeling.

4.3.2 An ultimate classification of the barriers

Besides a purely formal appeal of the shortened notation. it also indicates, directly, which particles are exchanged when crossing some of the singular boundary lines. Due to this, the combinatorics of coloring becomes easier, simplifying also our ultimate understanding of the correspondence between the microscopic symmetries/asymmetries of the particle-particle repulsion and the structure

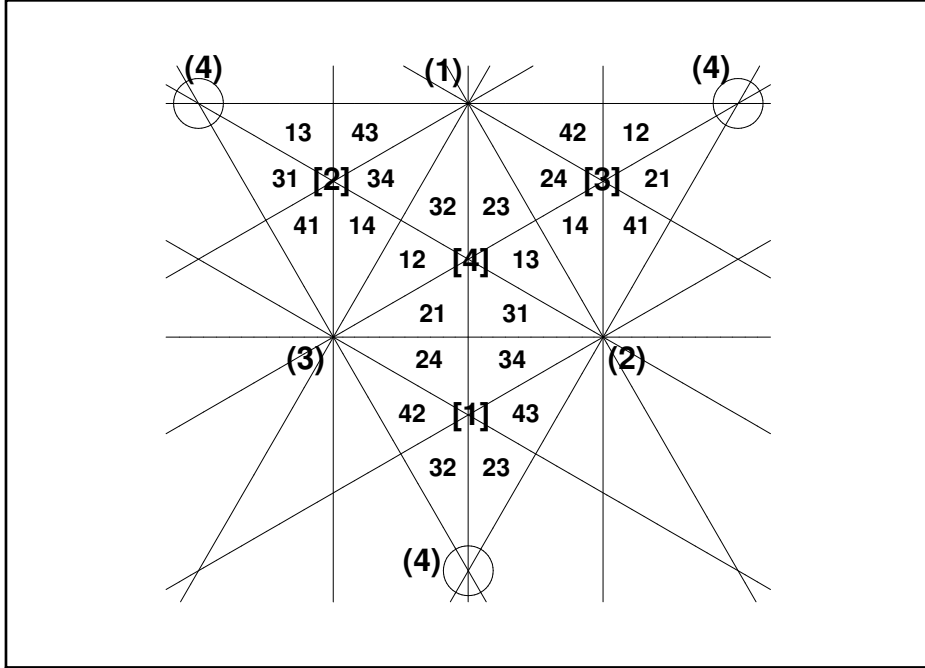


Figure 9: An alternative version of Figure 8 (a shortened Weyl-chamber classification).

of the macroscopic bound-state spectrum.

Any phenomenologically motivated and exhaustive “tetrahedral-surface” classification of all of the 24 Weyl chambers (and of their shared singular boundaries) as provided by Figures 8 and 9 can be reinterpreted as a completion of Figure 7, with its “invisible” half added. The four-digit particle orderings $ijkl$ of Figure 7 were shortened to the three-digit symbols bcd in Figure 8. The reason is that for the full identification of the chambers $W_{\{ijkl\}d}$ in our notation, the knowledge of the trailing triplet jkl is sufficient. The “missing” value of i (always equal to 1, 2, 3 or 4) coincides with the one given in the parenthesized symbol (i) marking the adjacent vertex. The validity of this coincidence can immediately be checked by the inspection of the “incomplete” Figure 7.

An alternative to Figure 8 is presented in Figure 9 where the remaining four “anonymous” sextuple intersections of the singularity lines (localized in the centers of the sides of the tetrahedron) are marked by the symbols [1], [2], [3] and [4]. Again, having noticed that the adjacent chambers-marking triplets of integers jkl share the vertex $[z]$ with $z \equiv l$, we introduced our ultimate index-shortening convention $jkl \rightarrow jk$ in Figure 9.

Under the latter convention one can finally decide to set the tetrahedron’s edges equal to one and to distinguish, subsequently, between the “long”, “middle” and “short” Weyl-chamber singular boundaries of the respective lengths $\alpha = 1/\sqrt{3} \approx 0.577$, $\beta = 1/2$ and $\gamma = 1/\sqrt{12} \approx 0.289$. Using this notation one can conclude that among the total number of 36 singular boundaries we have to deal here with 12 short ones, 12 middle ones and 12 long ones, with the long ones

always having the end points of the form $(i)[l]$ while representing the lines of the reordering of the remaining two integers j and k in our ultimate chamber-classification scheme of Figure 9.

5 Summary

One of the characteristic features of the conventional Calogero model (1) which describes the one-dimensional motion of a system of A quantum particles is the symmetry of the Hamiltonian with respect to the reordering of the particles. Remarkably enough, such a symmetry can be spontaneously broken because the details of the dynamics are such that whenever one fixes the ordering in advance, it will be, during the evolution, conserved. The system can be perceived as composed of multiple (i.e., of as many as $A!$) independent subsystems.

In such a situation it was natural to ask the question about the feasibility of breaking the above-mentioned symmetry manifestly. The motivation looked sound: In the symmetric model the spectrum was multiply degenerate and it was not too clear how one could unfold this degeneracy. At the same time, a promising methodical guidance seemed to lie in a manifest violation of the symmetry in a way illustrated by Figure 1 and by the “validating” small- A examples as thoroughly described in sections 2 and 3 above.

Along this line we found and described one of the possible answers. A modification of the model has been proposed in which the class of the forces which control the evolution has been extended. The basic idea of the innovation may be seen in the dynamical nature of the conservation of the ordering. It appeared to be caused by the original Calogero’s particle-particle-repulsion forces which were simply too strong. Their strength made any exchange of the neighboring particles prohibited.

We argued that the main reason of a complete suppression of the rearrangements had to be seen, first of all, in the strongly singular behavior of the Calogero’s original repulsion forces at short distances. From this we deduced that the whole rearrangement suppression paradox can be identified as a mere misunderstanding. We believe that the puzzle is now clarified.

We recollected that the conventional interpretation of the Calogero’s quantum system (as currently accepted by the majority of authors) is that its Hamiltonian H is a direct sum of all of the eligible ordering-dependent operators H_a where the subscript $a = \{i_1, i_2, \dots, i_A\}$ denotes and defines such an ordering. We imagined that from this point of view one can and should reinterpret the singular particle-particle repulsion as an impenetrability of the boundaries of the Weyl chambers W_a .

This was a decisive step. It gave birth to the main idea of our present paper: We proposed that one can construct a fairly large family of the new Calogero-like Hamiltonians in which a central role is played by the turn of our model-building attention from the complete kinematical Euclidean

space \mathbb{R}^A (comprising all of the individual particle coordinates $x_j \in \mathbb{R}$ with $j = 1, 2, \dots, A$) to its decomposition into a union of the *ad hoc* A -dimensional submanifolds.

Routinely, after the standard and trivial decoupling of the independent center-of-mass motion, the decomposition was reduced to the space \mathbb{R}^{A-1} defined as a union of the $(A - 1)$ -dimensional wedge-shaped Weyl chambers W_a . Then, the rest and the largest part of the paper had to be devoted to an explicit description and discussion of some consequences of the main idea.

One of the phenomenologically most interesting consequences of the decomposition of the set $\mathbb{R}^{A-1} = \bigcup W_a$ parametrized by the $(A - 1)$ -plet of relative coordinates concerned the boundaries between the neighboring Weyl chambers. These (repulsive) boundaries just correspond, from the microscopic point of view, to the mutual (repulsive) particle-particle interactions. Thus, in the language of mathematics, both of these representations of the (impenetrable) boundaries (not admitting any tunneling) appeared to be allowed left-right asymmetric.

The consequences of asymmetrization of such an “input” information about dynamics were discussed, in detail, at $A = 2$, $A = 3$ and at $A = 4$. In all of these exemplifications the loss of symmetry was shown to lead to a higher flexibility (which is due to the emergence of many new and freely variable parameters) as well as to a partial or complete suppression of the “global” degeneracy of the spectrum of the original Calogero’s model.

One of the most important challenges appeared to be the preservation of the exact solvability of the model after its asymmetrization. Due to an (at least partial) suppression of the degeneracy of the spectrum of the conventional symmetric model the related unfolding of the wave functions was, really, expected to prove useful, say, during some further future amendment of the model using, say, perturbation theory.

In our text we pointed out that in the symmetric-model special case the exact solvability of quantum Hamiltonian (1) is a nontrivial consequence of its Lie-algebraic symmetry [1]. The existence of this symmetry has only been rendered possible by the idealized picture of dynamics: The motion of the multiplet of particles is one-dimensional. Moreover, the mutual two-body interactions between individual particles are represented by the quartic plus inverse quartic potentials $V_{ij}^{(attractive)} \sim (x_i - x_j)^2$ and $V_{ij}^{(repulsive)} \sim 1/(x_i - x_j)^2$, respectively. In our present paper, from this point of view, the generalization can be simply characterized as making the shape of the forces $V_{ij}^{(repulsive)}$ asymmetric, i.e., different for $x_i > x_j$ and for $x_i < x_j$. This rendered the new Calogero-like model multi-parametric.

Another important aspect of the innovation is that in spite of the emergence of new free parameters, the resulting Calogero-like model remained solvable exactly. Although such a statement may sound surprising, the explanation is not too difficult, requiring just a more consequent use of the concept of the Weyl chambers. Incidentally, we could borrow their definition from the conventional Calogero’s model. Thus, what we only had to add was the emphasis upon the strongly singular nature of the particle-particle short-range interactions $V_{ij}^{(repulsive)}$. We only had to reread

the well known impenetrability of these barriers as a ban of particle exchanges.

During the unitary time-evolution of our generalized quantum system the ordering of the particles can be perceived as conserved. This is the most immediate consequence of the full-scale suppression of the tunneling between the neighboring Weyl chambers. Thus, any bound state of any Calogero-like quantum system can be understood as represented by the wave function supported by a single Weyl-chamber subdomain of coordinates. The only difference between the original and the present (i.e., “asymmetrized”) models is that in the former case, due to the uniqueness of their coupling C , every bound-state energy level is particle-ordering-independent.

We have shown how the “global” degeneracy of the levels can systematically be removed. What is sufficient is that in Hamiltonian (1) the coupling constant C is made configuration-dependent. Thus, along all of the inner boundaries of one of the Weyl chambers (say, of W_a characterized by the arrangement $x_{i_1} < x_{i_2} < \dots < x_{i_A}$ of the particle coordinates) we require that $C = C_a$ while in another Weyl chamber (say, in W_b characterized by another ordering $x_{j_1} < x_{j_2} < \dots < x_{j_A}$ *alias* permutation of the particles) we set $C = C_b$, etc. In general, one then has to distinguish between two scenarios. Either the respective singular coupling strengths coincide (i.e., we have $C = C_a = C_b$) or not.

In the latter case of our present interest we had to generalize, “asymmetrize” the form of the Hamiltonian of Eq. (1) by making it configuration-dependent. In particular, once we wished to keep the model solvable, we had to make *all* of the choices of the parameters mutually compatible. In this context, we found the criterion. Naturally, for an ultimate explicit construction of the solvable multiparametric Calogero-like new model, such a guarantee is a crucial mathematical ingredient. So we showed that such a guarantee is just a combinatorial exercise, provided only that we take into consideration the impenetrability of the singular particles-separating barriers.

The absence of tunneling enabled us to infer that the conventional Calogero’s choice of the spatially symmetric *alias* particle-exchange invariant $V_{ij}^{(repulsive)} \sim 1/(x_i - x_j)^2$ is not sufficiently general. In a systematic search for its more general spatially asymmetric and configuration-dependent alternatives we started our analysis at the two-particle scenario. We replaced the conventional Calogero’s choice of repulsion by the spatially asymmetric formula (8) and outlined the consequences. At $A = 3$ we displayed all of the six wedge-shaped Weyl chambers in Figure 3. In subsequent Figure 4 we showed that and how the two-dimensional Weyl-chamber wedges can be projected, for simplification purposes, on the segments of an auxiliary circle or on the sides of an auxiliary triangle. The idea has subsequently been transferred to $A = 4$. We emphasized that the role of the circle and triangle at $A = 3$ becomes inherited by a sphere and a cube or, alternatively, by a tetrahedron at $A = 4$, etc. This was our last illustration and argument in support of the consistency of the process of asymmetrization at any A .

Summarizing, we established, first of all, that what can and should be asymmetric are the boundaries between the Weyl chambers. Secondly, we emphasized that a return to the generic

form of the Calogero's Hamiltonian (1) is possible, provided only that this operator is reinterpreted as particle-ordering-dependent. Thirdly, its form of a direct sum over $A!$ subsystems has been shown to open the possibility of an unfolding of the “global” spectral degeneracy. Last but not least we pointed out that due to the absence of tunneling, the unfolding of levels can be mediated simply by the choice of a suitable multiplet of the particle-repulsion couplings $C_{\{i_1, \dots, i_A\}}$, leading to a classification via coloring of the Weyl chambers. For a really elementary illustration a return to Figure 1 can be, once more, recommended.

References

- [1] Olshanetsky, M. A.; Perelomov, A. M. Quantum completely integrable systems connected with semi-simple Lie algebras. *Lett. Math. Phys.* **1977**, *2*, 7 - 13.
- [2] Olshanetsky, M. A.; Perelomov, A. M. Quantum integrable systems related to Lie algebras. *Phys. Rept.* **1983**, *94*, 313 - 404.
- [3] Turbiner, A. Hidden algebra of the N-body Calogero problem. *Phys. Lett.* **1994**, *B 320*, 281 - 286.
- [4] Calogero, F. Solution of a three-body problem in one dimension. *J. Math. Phys.* **1969**, *10*, 2191 - 2196.
- [5] Calogero, F. Ground state of a one-dimensional N-body problem. *J. Math. Phys.* **1969**, *10*, 2197 - 2200.
- [6] Calogero, F. Solution of the one-dimensional N-body problem with quadratic and/or inversely quadratic pair potentials. *J. Math. Phys.* **1971**, *12*, 419 - 436.
- [7] van Diejen, J. F.; Vinet, L. (Eds.) *Calogero-Moser-Sutherland Models* (CRM Series in Mathematical Physics); Springer: New York, 2000.
- [8] Rühl, W.; Turbiner, A. V. Exact solvability of the Calogero and Sutherland models. *Mod. Phys. Lett.* **1995**, *A 10*, 2213 - 2222 (hep-th/9506105).
- [9] Sutherland, B. *Beautiful Models: 70 Years of Exactly Solved Quantum Many-Body Problems*; World Scientific: Singapore, 2004.
- [10] Polychronakos, A. P. Physics and mathematics of Calogero particles. *J. Phys. A: Math. Gen.* **2006**, *39*, 12793 (arXiv:hep-th/0607033).

- [11] Calogero, F. Calogero-Moser system. *Scholarpedia* **2008**, *3*, 7216.
Available online: http://www.scholarpedia.org/article/Calogero-Moser_system (accessed on 27 November 2023).
- [12] Ghosh, P. K.; Khare, A.; Sivakumar, M. Supersymmetry, shape invariance, and solvability of A_{N-1} and BC_N Calogero-Sutherland model. *Phys. Rev.* **1998**, *A 58*, 821.
- [13] Khastgir, S. P.; Pocklington, A. J.; Sasaki, R. Quantum Calogero-Moser Models: Integrability for all Root Systems. *J.Phys. A: Math. Gen.* **2000**, *33*, 9033 - 9064 (hep-th/0005277).
- [14] Boreskov, K. G.; Turbiner, A. V.; Vieyra, J. C. L. Solvability of the Hamiltonians related to exceptional root spaces: rational case. *Commun. Math. Phys.* **2005**, *260*, 17 - 44.
- [15] Dunkl, C. F.; Hu, Y. *Orthogonal polynomials of several variables*; Cambridge University Press: Cambridge, 2001.
- [16] van Diejen, J. F. Confluent hypergeometric orthogonal polynomials related to the rational quantum Calogero system with harmonic confinement. *Commun. Math. Phys.* **1997**, *188*, 467 - 497 ([q-alg/9609032]).
- [17] Chung, W. S.; Hassanabadi, H. One-dimensional quantum mechanics with Dunkl derivative. *Mod. Phys. Lett.* **2019**, *A 34*, 1950190.
- [18] Sedaghatnia, P.; Hassanabadi, H.; Junker, G.; Kříž, J.; Hassanabadi, S.; Chung, W. S. Investigation of the generalised Wigner-Dunkl harmonic oscillator and its coherent states. *Ann. Phys. (NY)* **2023**, *458*, 169445.
- [19] Scholtz, F. G.; Geyer, H. B.; Hahne, F. J. W. Quasi-Hermitian Operators in Quantum Mechanics and the Variational Principle. *Ann. Phys. (NY)* **1992**, *213*, 74–101.
- [20] Znojil, M.; Tater, M. Complex Calogero model with real energies. *J. Phys. A: Math. Gen.* **2001**, *34*, 1793 - 1803 (arXiv:quant-ph/0010087).
- [21] Znojil, M.; Tater, M. Exactly solvable three-body Calogero-type model with translucent two-body barriers. *Phys. Lett.* **2001**, *A 284*, 225 - 230.
- [22] Ghosh, P. K.; Gupta, K. S. On the real spectra of Calogero model with complex coupling. *Phys. Lett.* **2004**, *A 323*, 29 - 33 (arXiv:hep-th/0310276).
- [23] Assis, P. E. G.; Fring, A. From real fields to complex Calogero particles. *J. Phys. A: Math. Gen.* **2009**, *42*, 425206 (arXiv:0907.1079 [hep-th]).

- [24] Fring, A.; Smith, M. Antilinear deformations of Coxeter groups, an application to Calogero models. *J. Phys. A: Math. Gen.* **2010**, *43*, 325201 (arXiv:1004.0916 [hep-th]).
- [25] Bagarello, F.; Gazeau, J.-P.; Szafraniec, F.; Znojil, M. (Eds.) *Non-Selfadjoint Operators in Quantum Physics: Mathematical Aspects*; Wiley: Hoboken, NJ, USA, 2015.
- [26] Znojil, M. PT symmetric harmonic oscillators. *Phys. Lett.* **1999**, *A 259*, 220 - 223.
- [27] Jakubsky, V. PT-symmetric Calogero-type model *Czechosl. J. Phys.* **2004**, *54*, 67 - 69.
- [28] Brihaye, Y.; Nininahazwe, A. On PT symmetric extensions of the Calogero model. *Int. J. Mod. Phys.* **2004**, *A 19*, 4391 - 4400 (arXiv:hep-th/0311081).
- [29] Fring, A.; Znojil, M. PT-symmetric deformations of Calogero models. *J. Phys. A: Math. Gen.* **2008**, *41*, 194010 (arXiv:0802.0624).
- [30] Fring A PT -symmetric deformations of integrable models. *Phil. Trans. Roy. Soc. Lond.* **2013**, *A 371*, 20120046 (arXiv:1204.2291).
- [31] Correa, F.; Lechtenfeld, O. Algebraic integrability of PT-deformed Calogero models. *J. Phys.: Conf. Ser.* **2021**, *2038*, 012007.
- [32] Jakubsky, V.; Znojil, M.; Luis, E. A.; Kleefeld, F. Trigonometric identities, angular Schrödinger equations and a new family of solvable models. *Phys. Lett.* **2005**, *A 334*, 154 - 159 (quant-ph/0410023).
- [33] Hakobyan, T.; Nersessian, A.; Yeghikyan, V. The cuboctahedric Higgs oscillator from the rational Calogero model. *J. Phys. A: Math. Theor.* **2009**, *42*, 205206 (arXiv:0808.0430 [hep-th]).
- [34] Feigin, M. V. Intertwining relations for the spherical parts of generalized Calogero operators. *Theor. Math. Phys.* **2003**, *135*, 497 - 509.
- [35] Hakobyan, T.; Lechtenfeld, O.; Nersessian, A. The spherical sector of the Calogero model as a reduced matrix model. *Nucl. Phys.* **2012**, *B 858*, 250 - 266 (arXiv:1110.5352 [hep-th]).
- [36] Feigin, M.; Lechtenfeld, O.; Polychronakos, A. The quantum angular Calogero-Moser model. *JHEP* **2013**, *1307*, 162 (arXiv:1305.5841[math-ph]).
- [37] Correa, F.; Lechtenfeld, O. The tetrahedric angular Calogero model. *JHEP* **2015**, *1510*, 191 (arXiv:1508.04925 [hep-th]).

- [38] Landau, L. D.; Lifshitz, E. M/ *Quantum Mechanics: Non-Relativistic Theory*; Pergamon: New York, 1977.
- [39] Lapointe, L.; Vinet, L. Exact Operator Solution of the Calogero-Sutherland Model. *Commun. Math. Phys.* **1996**, *178*, 425 - 152.
- [40] Znojil, M. Comment on conditionally exactly soluble class of quantum potentials. *Phys. Rev.* **2000**, *A 61*, 066101 (quant-ph/9811088).
- [41] Ishkhanyan, A. M. Conditionally exactly solvable Dirac potential, including $x^{1/3}$ pseudoscalar interaction. Int. conf. Analytic and algebraic methods in physics XX (FNSPE Prague, August 29, 2023, invited talk).
- [42] Ishkhanyan, A. M.; Kreinov, V. P. Exact solution of the 1D Dirac equation for a pseudoscalar interaction potential with the inverse-square-root variation law. *Sci. Rep.* **2023**, *13*, 13482.
- [43] Ishkhanyan, A. M.; Kreinov, V. P. Conditionally exactly solvable Dirac potential, including $x^{1/3}$ pseudoscalar interaction. *Phys. Scr.* **2023**, *98*, 075229.
- [44] Flügge, S. *Practical Quantum Mechanics I*; Springer-Verlag: Berlin, 1971.
- [45] Post, G.; Turbiner, A. V. Quasi-solvability of Calogero-Sutherland model. *Russ. J. Math. Phys.* **1995**, *3*, 113.
- [46] A. V. Turbiner, A. V. Quasi-Exactly Solvable Hamiltonians related to Root Spaces. *J. Nonlin. Math. Phys.* **2005**, *12*, Suppl. 1, 660 - 675.
- [47] Brink, L.; Turbiner, A. V.; Wyllard, N. Hidden algebras of the (super) Calogero and Sutherland models. *J. Math. Phys.* **1998**, *39*, 1285 - 1315.
- [48] Boreskov, K. G.; Vieyra, J. C. L.; Turbiner, A. V. Solvability of the F4 integrable system. *Int. J. Mod. Phys.* **2001**, *A 16*, 4769-4801.
- [49] Humphreys, J. E. *Reflection groups and Coxeter groups*; Cambridge University Press: Cambridge, 1990.
- [50] Coxeter, H. S. M. *Regular Polytopes* (3rd ed.); Dover Publications: New York, 1973.
- [51] Available online: https://commons.wikimedia.org/wiki/File:Disdyakis-6_spherical.png (accessed on 27 November 2023).
- [52] Available online: <https://en.wikipedia.org/wiki/File:Tetrakisshexahedron.jpg> (accessed on 27 November 2023).

- [53] Available online: https://commons.wikimedia.org/wiki/File:Disdyakis_6_in_rhombic_6.png (accessed on 27 November 2023).
- [54] Brink, L.; Hansson, T. H.; Vasiliev, M. Explicit solution to the N body Calogero problem. *Phys. Lett.* **1992**, *B 286* 109 - 111, [[hep-th/9206049](#)].

Appendix: The occurrence of asymmetric impenetrable barriers in relativistic quantum mechanics

The conventional non-relativistic quantum theory admits, in contrast to its classical limit, the existence of bound states even in a strongly singular attractive potential $V(x) = -g^2 X^{-2}$, provided only that the coupling is not too large [38]. In paper [43], Ishkhanyan with Krainov turned attention to analogous singular-potential problems in relativistic quantum mechanics. Some of their results might find a not quite expectable non-relativistic counterpart in our present paper.

In their study of a stationary one-dimensional Dirac equation they considered, in particular, a specific pseudoscalar screened Coulomb potential exhibiting a conventional spatial symmetry,

$$W^{(IK)}(x) \sim a |x|^{-1} + b |x|^{+1/3}.$$

In a way reported during recent conference [41] they revealed that besides its well motivated phenomenological origin, the model could also prove methodically relevant because it can be made conditionally exactly solvable (CES; for a concise information on the latter concept see also our older comment [40]).

From our present point of view the essence of the Ishkhanyan's and Krainov's message is that after one rewrites Dirac equation in a mathematically equivalent non-relativistic bound-state form, one just has to solve the effective Schrödinger equation with a spatially manifestly asymmetric potential

$$V^{(IK)}(x) = \begin{cases} (x^2)^{1/3} + u_{Left}^{(IK)}/x^2, & u_{Left}^{(IK)} = \ell(\ell + 1) > 0, & x < 0, \\ (x^2)^{1/3} + v/(x^2)^{1/3} + u_{Right}^{(IK)}/x^2, & u_{Right}^{(IK)} = -\ell(-\ell + 1) < 0, & x > 0 \end{cases} \quad (23)$$

with parameter $\ell \in (0, 1)$. In particular, their model possessed a spatially manifestly asymmetric central singularity with which the mathematically desirable CES property has been found to occur at a special value of $\ell = \ell^{(IK)} = 1/6$.

We have to add that the authors of paper [43] worked with an extreme, phenomenologically ambitious asymmetry of their potential. In our present notation they used just Eq. (8) with two independent couplings,

$$\ell_{(left)}(\ell_{(left)} + 1) = \frac{7\hbar^2}{72m}, \quad \ell_{(right)}(\ell_{(right)} + 1) = -\frac{5\hbar^2}{72m}. \quad (24)$$

They were of an opposite sign and of different sizes, and there were no free parameters left. Indeed, once we return to the units $\hbar = 2m = 1$, their CES constraint (24) acquired the form of our present Eq. (10) with $y = y_{(CES)} = 1/6$.

For us, the latter results were encouraging. Demonstrating that it makes sense to work with asymmetric singular forces. By relations (24) we also felt inspired to a replacement of ansatz (8)

by the more elementary one-parametric convention (11). We came to the conclusion that the CES-based necessity of working with a fixed value of $\ell = 1/6$ in (24) was too high a price for the technical advantage of the user-friendliness of the model. Thus, we turned attention to the harmonic-oscillator confinement (11) because qualitatively, the asymmetric shape of our two-body potentials as sampled by Figure 1 is, after all, not too different from the shape of the CES potential $V_{CES}^{(IK)}(x)$ of Eq. (23) as displayed in Figure Nr. 2 of paper [43].

In [41] the authors emphasized that it makes good sense to search for a deeper understanding of the connection between the flexibility of the spectral properties and the absence of the tunneling caused by the singular nature of the X^{-2} barriers. They noticed that the choice of the matching condition at $X = 0$ “must be adjusted according to the specific physical context under consideration” [43]. In our present paper the latter point has attracted due attention. We managed to disentangle several related technical challenges. In particular, we shortened the argumentation by omitting all of the phenomenologically motivated references to the relativistic quantum dynamics. After all, even in [43] we read that the “results show a significant difference between the Schrödinger and Dirac cases”, and that “it is clear that the reason for the discrepancy [between the Schrödinger and Dirac models] is that the boundary conditions we [=they] use for these two cases are [different, i.e.,] due to different considerations”. For this reason we kept the scope of our present study restricted to the strictly non-relativistic systems, promising still a very broad potential applicability [11].